Numerical Analysis of Wideband and High Directive Bowtie THz Photoconductive Antenna

Amira Dhiflaoui [1], Ali Yahyaoui [1,2], Jawad Yousaf [2,3], Shahid Bashir [4], Bandar Hakim [2], Toufik Aguili [1], Hatem Rmili [1,2], and Raj Mittra [2,5]

[1] University of Tunis El Manar (UTM), National Engineering School of Tunis (ENIT)
Communications Systems Laboratory (SysCom), BP 37, Belvédère 1002 Tunis, Tunisia

[2] Electrical and Computer Engineering Department, Faculty of Engineering, King Abdulaziz University
P.O. Box 80204, Jeddah 21589, Saudi Arabia

[3] Department of Electrical and Computer Engineering, Abu Dhabi University, United Arab Emirates
hmrmili@kau.edu.sa

[4] Department of Electrical Engineering, University of Engineering & Technology, Peshawar, Pakistan

[5] Electrical and Computer Engineering Department, University of Central Florida, EMC Lab, Orlando, FL 32816 USA

Abstract – This paper presents a novel wideband and high directivity Bowtie photoconductive antenna (PCA) for THz frequency applications. The radiation properties of proposed PCA were analyzed by varying important design parameters, such as substrate thickness, conductor thickness, bowtie antenna width, length and gap. The optimized values of these parameters are then used to design a wideband PCA THz antenna which exhibits impedance bandwidth of 3 THz, 3 dB AR bandwidth of 6 THz, peak directivity of about 18.2 dBi and peak radiation efficiency of 98% within the operating band. To improve the directivity of the proposed antenna, a silicon-based lens is added in the structure and the effect of silicone lens on THz antenna directivity is also studied for enhanced directivity of proposed antenna. The proposed THz antenna can be a prospective candidate for future THz applications such as spectroscopy, imaging, sensing and indoor communication.

Index Terms – Bowtie antenna, high directivity, photoconductive THz antenna, wideband.

I. INTRODUCTION

Due to an increased demand for high data rate and wide bandwidth applications there has been a consistent trend of moving towards higher frequency bands in the electromagnetic spectrum. The recent emergence of 5G technology has commercialized the use of millimeter waves (30GHz to 300GHz) for high data rate communication [1-3]. Now, there has been an ongoing attempt to use THz waves or submillimeter waves having

frequency from 0.3 THz to 10 THz for specialized applications like brain imaging, tumor detection, security screening, material characterization using spectroscopy, bio-sensing, high data rate indoor communication and non-invasive imaging [4-9].

However, antenna design for THz is a big challenge in itself. Antenna design techniques used at low frequency are not applicable at THz range. Due to very small operating wavelength, the size of antenna becomes very small making it impossible to feed such an antenna using conventional feeding mechanism [3]. However, loss in THz signal power as it propagates is a serious challenge. This necessitates high gain THz antenna to compensate the losses and polarization insensitivity characteristics, particularly for imaging and sensing applications.

THz antennas working on the principle of photoconduction are getting attention by researchers working in the field of THz systems. However, their limitation is reduced radiated THz power and thus low efficiency [10-12]. Also, as compared to microwave antennas THz antennas require different excitation and current generation process that involve losses. A wideband on-chip dielectric resonator antenna (DRA) operating at sub-THz frequencies was proposed with a bandwidth of 65 GHz [4]. Low directivity is another constraint in THz antenna design. A bowtie-shaped antenna combined with a silicon-based lens and with an artificial magnetic conductor (AMC) was proposed to enhance its directivity properties [5]. The other reported examples of THz PCA designs are dipole planner array [13], Yagi-Uda [14], bow tie [11, 12, 15, 16], conical

horn [17] and spiral-shaped [18]. The authors used the antireflection coatings [11, 19], integration of lens [11, 12, 20-23] and metasurfaces [5, 13, 15] with antenna structures to enhance THz antennas directivity.

In this paper we have proposed a novel ultra wideband (UWB) and high directivity bowtie photoconductive antenna for THz band. The radiation properties of proposed antenna have been optimized after parametric analysis of critical design parameters. From full-wave EM simulations, the proposed antenna achieves the -10 dB impedance bandwidth of 3 THz with peak gain of about 15 dBi and radiation efficiency of 98% within the operating band. The antenna exhibit impedance matched behavior across 2 THz to 5 THz band. The directivity of antenna has also been enhanced using lens with optimized design parameters. The design, shape and structure of the added lens is selected carefully to ensure the wideband operation as well as improved directivity from the realized design. The designed antenna shows superior performance in terms of impedance bandwidth and efficiency as compared to the designs proposed in [10-18]. The detailed analysis of the design procedure, parametric study, effect of the added lens on the antenna performance and discussion about the obtained results is given in the following sections.
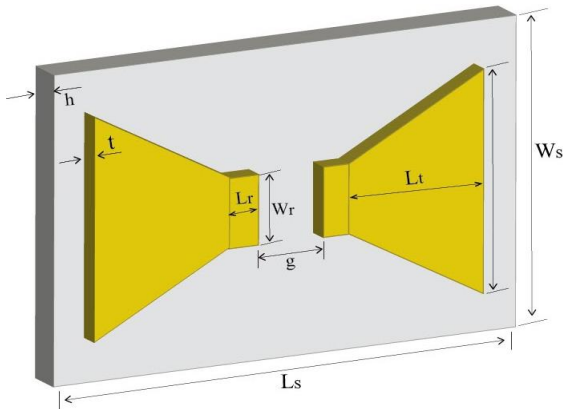
II. DESIGN PROCEDURE

A. Antenna design

The proposed antenna design is shown in Fig. 1. It is basically a bowtie antenna printed on a photoconductive substrate. DC bias is applied across the bowtie antenna. In order to generate THz radiation from this bowtie antenna, optical pulse is incident on the antenna gap (g), which propagates into the photoconductor and generate photocarriers inside the photoconductor. The generated photocarriers are accelerated in the DC bias field, producing a transient photocurrent, which drives the bowtie antenna and ultimately re-emits as a THz frequency pulse [24]. The metal conductor of the designed bowtie antenna has thickness of 't' and is made of gold conductor whereas the substrate is made of quartz. The relative permittivity and loss tangent of the used substrate material is 3.78 and 0.0001, respectively. The full-wave numerical analysis of the proposed bowtie THz antenna is performed in CST MWS. The initial dimensions of the designed antenna are given in Table 1.

In order to increase the directivity of this antenna a hemispherical lens is placed on bottom side as shown in Fig. 2.
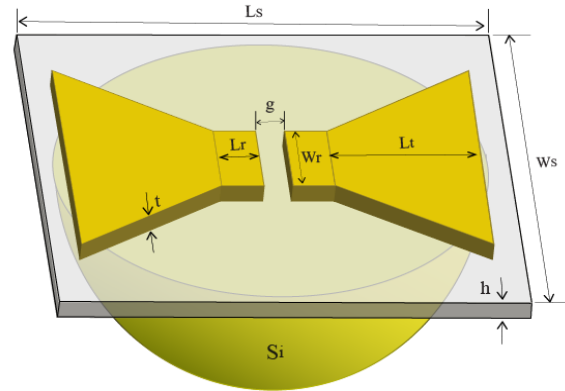

Fig. 2. Design of Bowtie THz antenna with lens.

Fig. 1. Design of bowtie THz antenna.

Table 1: Initial design dimensions of Bowtie THz antenna

Parameters	Values (μm)
L_s	347
h	1.3
t	0.02
W_s	340
L_t	103
W_t	220
W_r	7
L_r	12
g	7.6

B. Optimization of the UWB THz antenna

Firstly, the parametric analysis of the antenna design parameters of Fig. 1 is performed to obtain the optimized design parameters for the ultra-wideband (UWB) impedance matching characteristics. The major issues in the modeling are about the extensive analysis of the effect of the different antenna design parameters on its performance. For this purpose, a parametric analysis was performed to obtain the optimized design parameters for the ultra-wideband impedance matching characteristics. The variation ranges of the various design parameters for the parametric study are selected carefully keeping in view the fabrication constrains to minimize the extensive memory requirements of the numerical models with various design parameters

The upper and lower limit of each parameter is chosen by covering the maximum range of values without affecting the shape of the proposed antenna. In all parametric analysis we present only the important parameters values which give us significant behavior keeping in view the fabrication constrains.

1) Effect of Substrate Thickness (h)

Because the thickness of the substrate (*h*) is usually larger than the wavelength of THz waves, surface/ substrate modes may be generated and the effect of the substrate cannot be ignored. For this purpose, parametric study was conducted by varying the substrate thickness from 1.3 µm to 4.3 µm. The effect on S_{11} is shown in Fig. 3. As thickness increases the impedance matching behavior slightly degrades at upper operating frequencies. The results depict that for the optimal value of substrate thickness, *i.e.*, 2.3 µm, the -10 dB impedance bandwidth of the designed antenna is around 3 THz (2 to 5 THz).
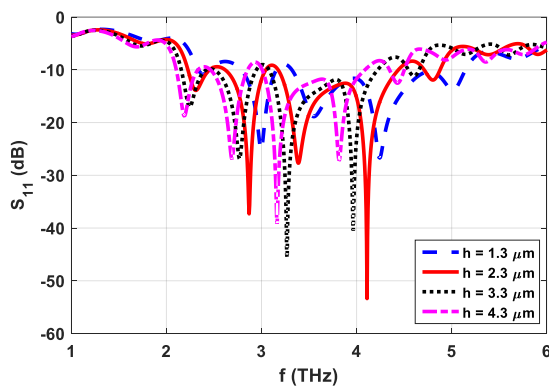

Fig. 3. S_{11} of THz antenna without lens with the variations in substrate thickness (*h*).

Normally, the antennas having -10 dB impedance bandwidth of greater than equal to 500 MHz or fractional bandwidth (FBW) of more than 20% are referred as ultra-wideband (UWB) antennas [25] [26]. As depicted in Fig. 3, the -10 dB impedance bandwidth ($|S_{11}| \leq -10\ dB$) and FBW of our proposed antenna is around 3 THz and 50% respectively, that's why we are using the term of UWB THz antenna for the proposed antenna structures.

2) Effect of Gold Thickness (t)

The effect of metal thickness (*t*) of top layer of proposed THz antenna is studied parametrically as shown in Fig. 4. The metal thickness is varied from 0.02 µm to 0.05 µm and only slight variation in the impedance matching characteristics across the band is observed.

3) Effect of L_s

The parametric study on L_s is also conducted and the variations in S_{11} are shown in Fig. 5 which depicts that

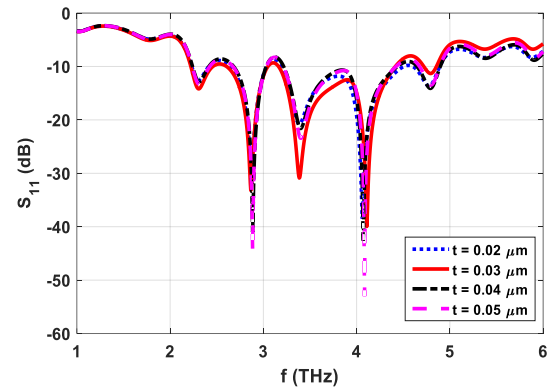this parameter has also no effect on S_{11} as like metal thickness variations.

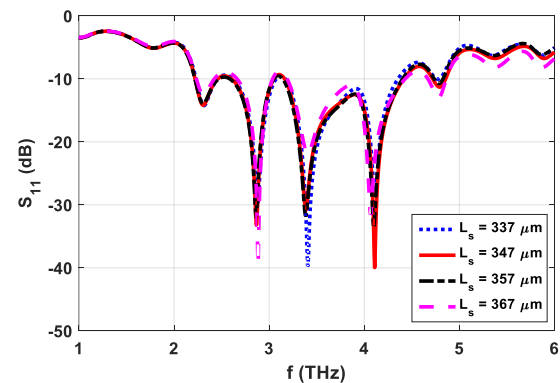Fig. 4. S_{11} of THz antenna without lens with the variations in metal thickness (*t*).

Fig. 5. S_{11} of THz antenna without lens with the variations in substrate length (L_s).

4) Effect of L_t

The effect of variation in L_t on antenna S_{11} is shown in Fig. 6. This parameter is varied from 103 µm to 124 µm and it is observed that matching behavior slightly drift towards lower frequency with increasing L_t values.
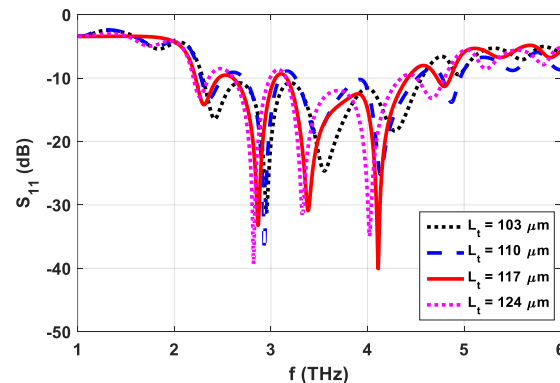

Fig. 6. S_{11} of THz antenna without lens with the variations in L_t.

5) Effect of W_r

As this parameter is varied between 7 µm to 19 µm, significant variation in S11 is observed as shown in Fig. 7. The best result is obtained for W_r =13 µm.
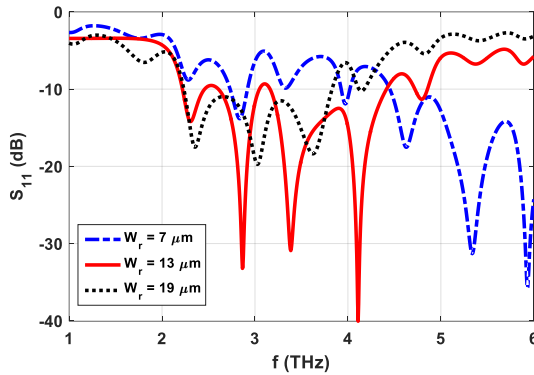

Fig. 7. S_{11} of THz antenna without lens with the variations in W_r.

6) Effect of Bowtie Aram Width (W_t)

The parameter W_t (bowtie arm width or flare angle) is varied from 220 µm to 280 µm. Figure 8 shows the effect of this variations on the reflection coefficient of the antenna. It can be noted from Fig. 8 results that the increase in W_t brings a minor shift (towards lower frequencies) in the resonance frequencies of the antenna.
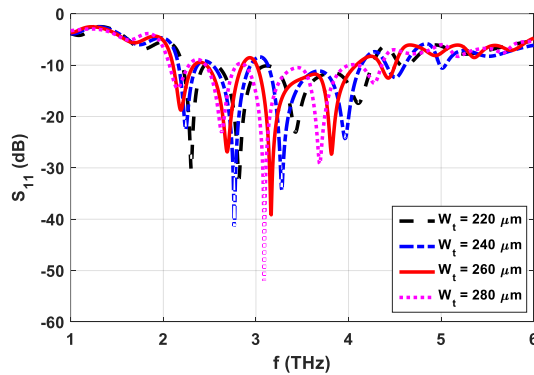

Fig. 8. S_{11} of THz antenna without lens with the variations in W_t.

7) Effect of Growth W_s

The change in reflection properties of the designed THz bowtie antenna when the parameter W_s (width of the substrate) is varied from 340 µm to 370 µm is depicted in Fig. 9. The change in the width of the substrate mainly effects the dips of the resonance frequencies without any significant change in the impedance bandwidth of the antenna.

8) Effect of g

The gap between the bowtie antenna poles is also varied from 1.6 µm to 7.6 µm to analyze its impact on

S_{11} characteristics as shown in Fig. 10. As the gap width is increased from 1.6 µm to 3.6 µm the impedance matching improved. However, when *g* is increased further the impedance matching started degraded again.

Table 2 lists the optimized design parameters of the proposed bowtie THz antenna based on the conducted parametric study. The performance of the antenna is further analyzed with the addition of the lens in the antenna structure with the optimized antenna parameters of Table 2.
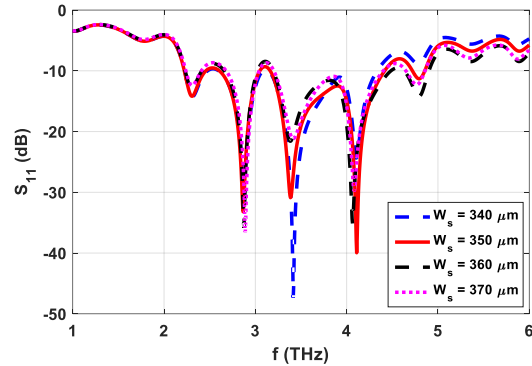

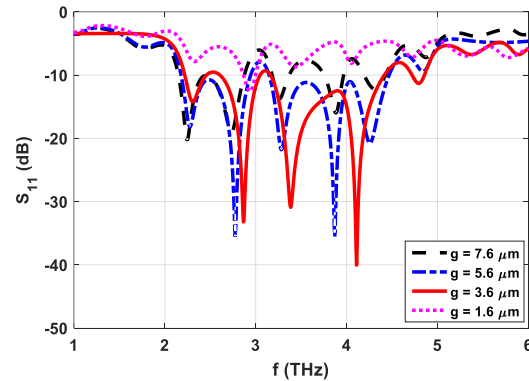Fig. 9. S_{11} of THz antenna without lens with the variations in W_s.

Fig. 10. S_{11} of THz antenna without lens with the variations in *g*.

Table 2: Optimized design dimensions of Bowtie THz antenna

Parameters	Values (µm)
L_s	347
h	2.3
t	0.03
W_s	350
L_t	117
W_t	260
W_r	13
L_r	8
g	3.6

III. ANALYSIS OF UWB THZ ANTENNA WITH LENS

This section describes the analysis of the change in the diameter (R_L) of the added silicon lens on the antenna performance. The performance of the antenna is analyzed in terms of the impedance matching, directivity, axial ratio and efficiency of the antenna. Following sections illustrates the conducted analysis.

A. Impedance matching

Figure 11 shows the variations in the reflection coefficient of the antenna when the diameter of the added silicon lens is changed from 80 µm to 160 µm with a step size of 40 µm. The results depict that the -10 dB impedance bandwidth of the proposed antenna improves with the increase in the diameter of the silicon lens.
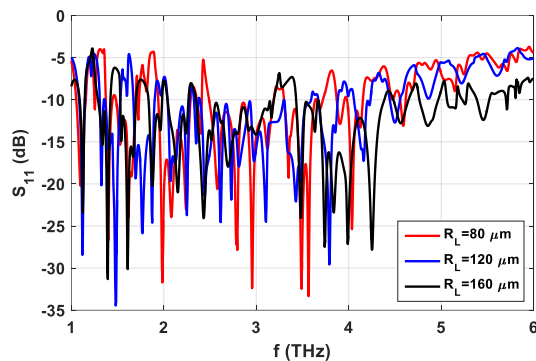

Fig. 11. Effect of variations in R_L on S_{11} of THz antenna with lens.

B. Directivity

In order to increase the directivity of proposed THz antenna, hemispherical silicone lens is placed over the bowtie antenna. The effect of radius of silicone lens on directivity is shown in Fig. 12. The best performance is observed for R_L =120 µm with consistently high directivity across the whole operating band. The directivity of the antenna decreases in higher frequency band when the diameter of the silicon lens is increased to 160 µm.
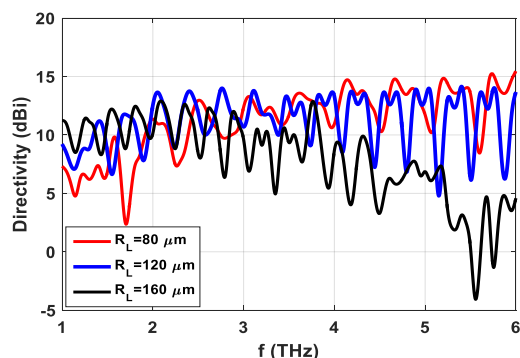

Fig. 12. Effect of variations in R_L on directivity of THz antenna with lens.

C. Axial ratio

In order to study the polarization behavior of proposed THz antenna, the axial ratio is observed for different values of R_L as shown in Fig. 13. The antenna generally exhibits linear polarization behavior. However, for R_L =160 µm circular polarization behavior is observed near 5.5 THz. It can be observed from the Fig. 13 that the 3 dB AR bandwidth of the proposed antenna is 6 THz.

The presence of the lens affects the polarization of the radiated electromagnetic fields because this lens generates a phase shift due to the wave propagation within it. This phase shift depends on the shape and the permittivity of the propagation medium constituting the lens, and thus explains the variation of the antenna polarization with the radius of the added lens. However, the polarization changes from linear to circular for a specific size of the lens means that the lens acts as a Quarter-Wavelength Plate (QWP) at certain frequency ranges, and the introduced phase shift is equal to $\pi/2$.
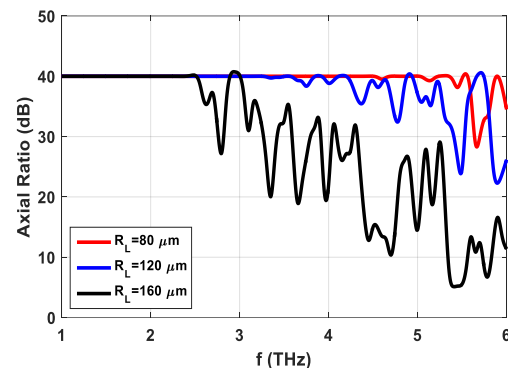

Fig. 13. Effect of variations in R_L on axial ratio of THz antenna with lens.

D. Efficiency

The effect of R_L on proposed THz antenna efficiency is also studied. Figure 14 shows the total efficiency results of the analyzed antenna for the three different diameters of silicon lens. The overall efficiency of the proposed antenna is more than 55% in the entire analyzed frequency band of 1 to 6 THz. The best efficiency is observed for R_L = 160 µm with peak value of 98%.

IV. RESULTS AND DISCUSSIONS

This section discusses the radiation pattern characteristics of the designed antenna with and without lens. The radiation pattern of proposed antenna was simulated for the three different values of RL. Figure 15 shows the 2D polar radiation pattern for R_L = 80 µm for proposed THz antenna with and without lens. It can be observed that lens significantly increased the directivity by focusing the radiation pattern towards it. The addition of the lens increases the level of the distributed current around the source location of the antenna which results in the enhancement of the infrared (IR) coupling and thus

the increase of the directivity of the antenna. The peak directivity for R_L =80 µm lens in both planes is given in Table 3.
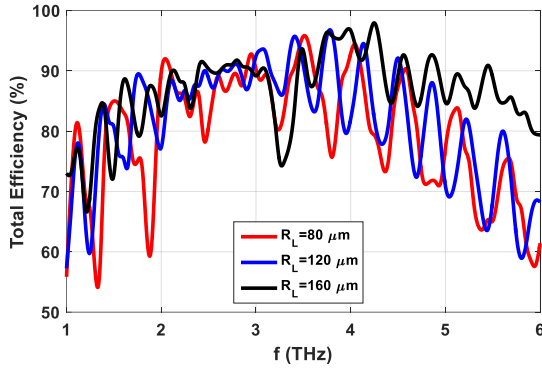

Fig. 14. Effect of variations in R_L on efficiency of THz antenna with lens.

Table 3: Increase of the antenna directivity (in dB) at different frequencies for R_L =80 µm

Frequency (THz)	Phi = 0º	Phi = 90 º
2	13.4	13.4
2.95	17.5	17.5
3.5	14.4	14.4
4.05	13.1	13.1

Figure 16 shows the 2D polar radiation pattern of the proposed THz antenna with and without lens with R_L =120 µm. Table 4 depicts the peak directivities of the designed antenna with lens which has diameter of 120 µm.

Table 4: Increase of the antenna directivity (in dB) at different frequencies for R_L =120 µm

Frequency (THz)	Phi = 0º	Phi = 90 º
1.75	18.2	18.2
2.1	15.7	15.7
3.8	16.6	16.6
4.5	11	11

The 2D polar radiation pattern of the analyzed antenna with (R_L =160 µm) and without lens is shown in Fig. 17 for different frequencies in both azimuth and elevation planes. Table 5 illustrates the increase in the peak directivity of the antenna with the addition of the lens in its structure.

The 3D patterns of proposed THz antenna with different size lens are given in Fig. 18. It can be noted from Fig. 18 that the radiation pattern is completely opposite-pointed. To increase the performance of the proposed antenna, a silicon lens is added on the backside of the structure. The structure was excited from the upper side and the target from the installed lens is to concentrate the main beam in the back side of the structure whereas reduce the lobes on the upper side. The highly directive main beam can easily be observed in all cases. It can be noted from Tables 3, 4 and 5 results that the maximum peak directivity of the designed antenna with lens diameter of 80 µm, 120 µm, and 160 µm is 17.5 dBi (@ 2.95 THz), 18.2 dBi (@ 1.75 THz) and 16.6 dBi (@ 2.15 THz). The directivity of the antenna increases with the enhancement of the lens diameter from 80 µm to 120 µm. However, a slight degradation in the directivity performance is observed with the further enhancement of the lens diameter to 160 µm.

V. COMPARISON WITH LEGACY DESIGNS

The comparison of the proposed wideband bowtie THz antenna with the available PCA designs in the literature is performed. The comparison of the proposed design is performed in terms of the antenna type, antenna substrate, antenna electrode material, lens type, -10 dB impedance bandwidth, maximum directivity, and 3dB AR bandwidth of the reported designs. The summary of the performed comparison with legacy designs in illustrated in Table 6. The authors in [10-12, 15, 17] used the hemispherical based silicon lenses to enhance the directivity of the proposed different kinds of antenna types. Malhotra et al. [13] and Zhu et al.[15] integrated the frequency selective surface (FSS) with the antenna electrodes to increase the directivity of the proposed dipole planner array and bow-tie PCAs, respectively. However, as can be noted from Table 6 that the reported maximum directivity of all compared legacy designs is less than the achieved peak directivity of proposed THz antenna. In addition, the -10 dB impedance and 3 dB AR bandwidth of the proposed bowtie antenna design is highest among all the compared legacy designs [10-18]. This comparison reflects that the proposed THz antenna can be a prospective candidate for future THz applications such as spectroscopy, imaging, sensing and indoor communication due to its wideband impedance and AR bandwidth characteristic as well as high directivity.

Table 5: Increase of the antenna directivity (in dB) at different frequencies for R_L =160 µm

Frequency (THz)	Phi = 0º	Phi = 90 º
1.6	16.4	16.4
2.15	16.6	16.6
2.45	14.8	14.8
3.75	15.7	15.7

Fig. 15. 2D radiation pattern for R_L =80 µm: (a) 2 THz, (b) 2.95 THz, (c) 3.5 THz, and (d) 4.05 THz.

(a)

(b)

(c)

(d)

Fig. 16. 2D radiation pattern for R_L =120 µm: (a) 1.6 THz, (b) 2.15 THz, (c) 2.45 THz, and (d) 3.75THz.
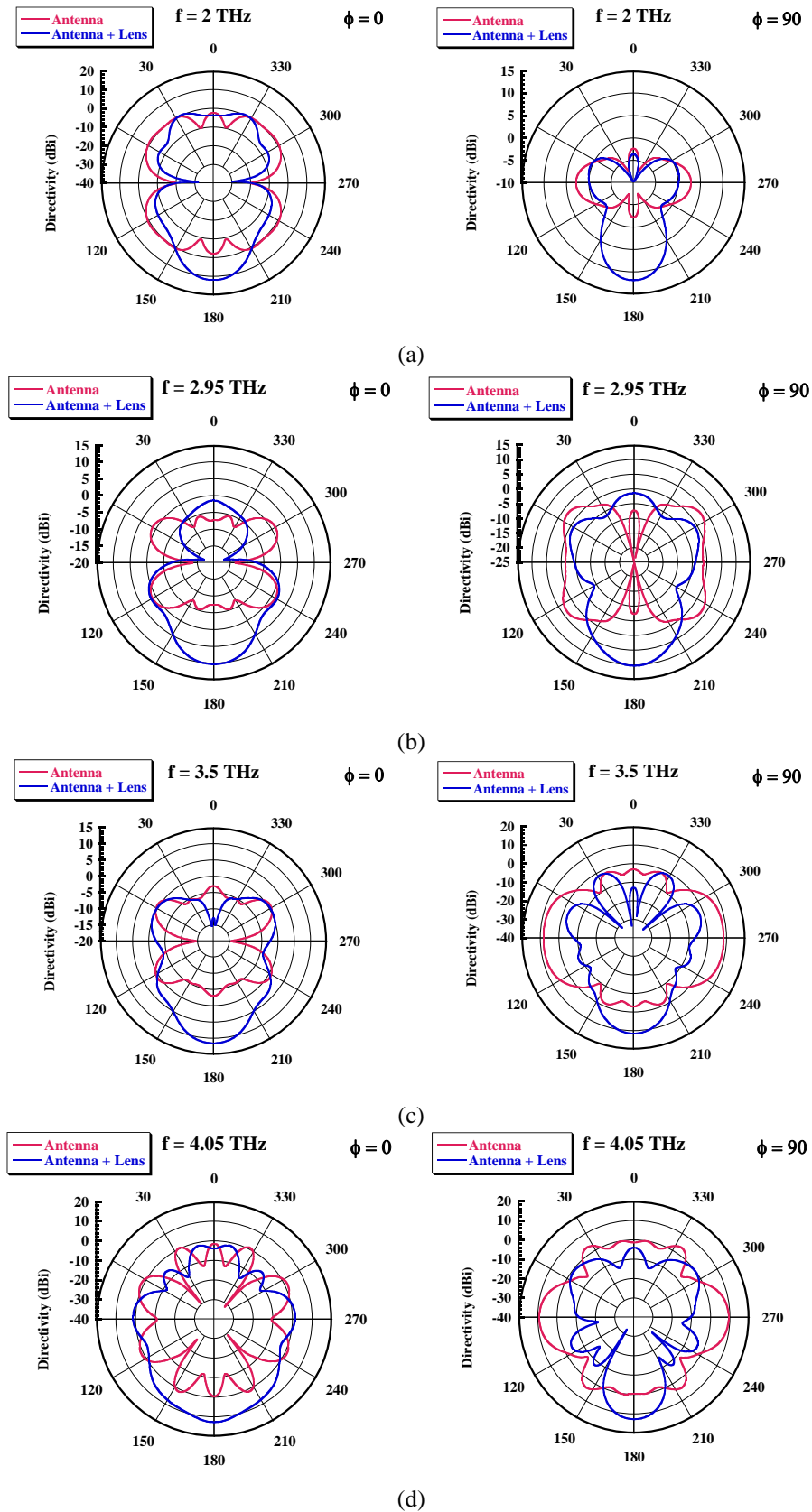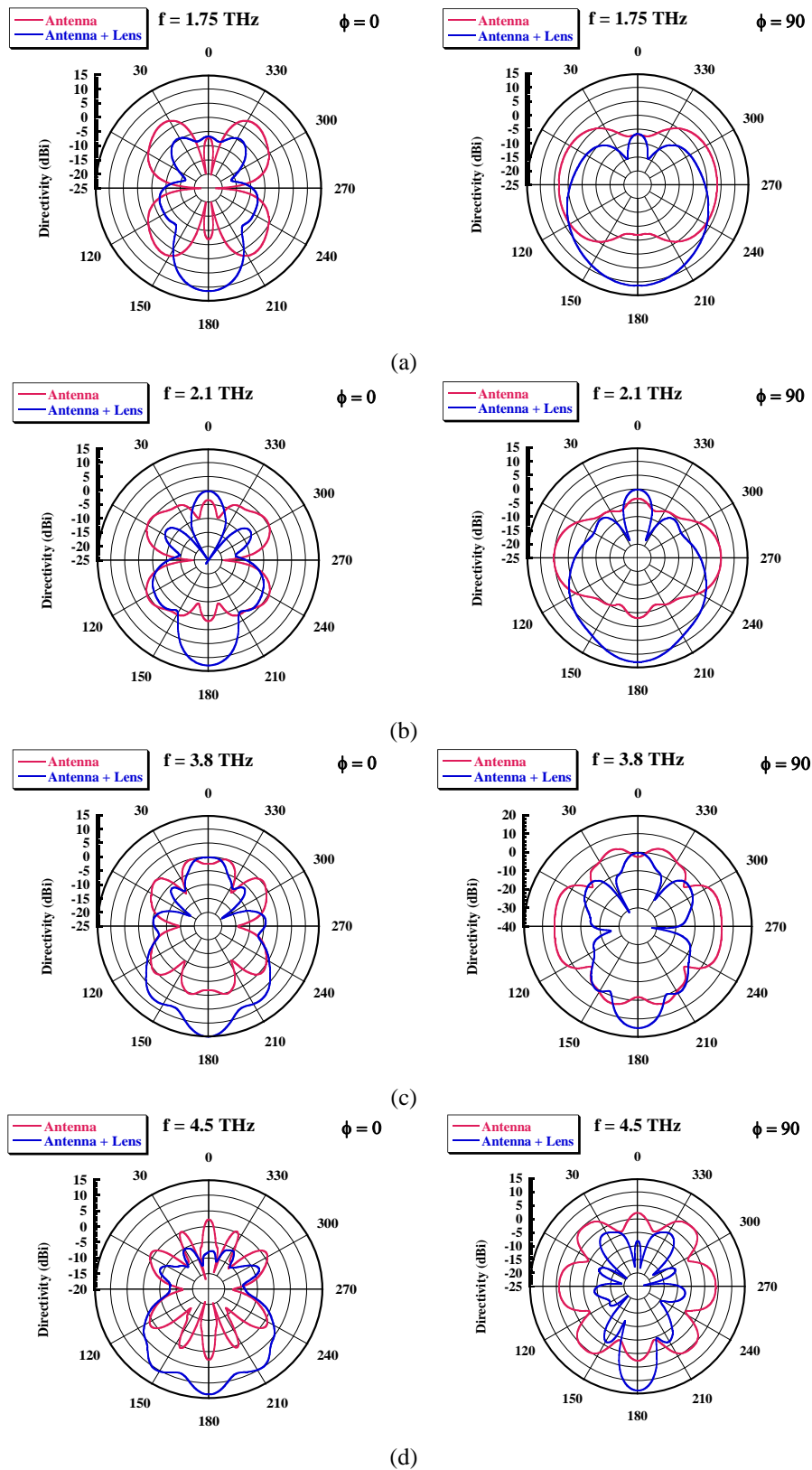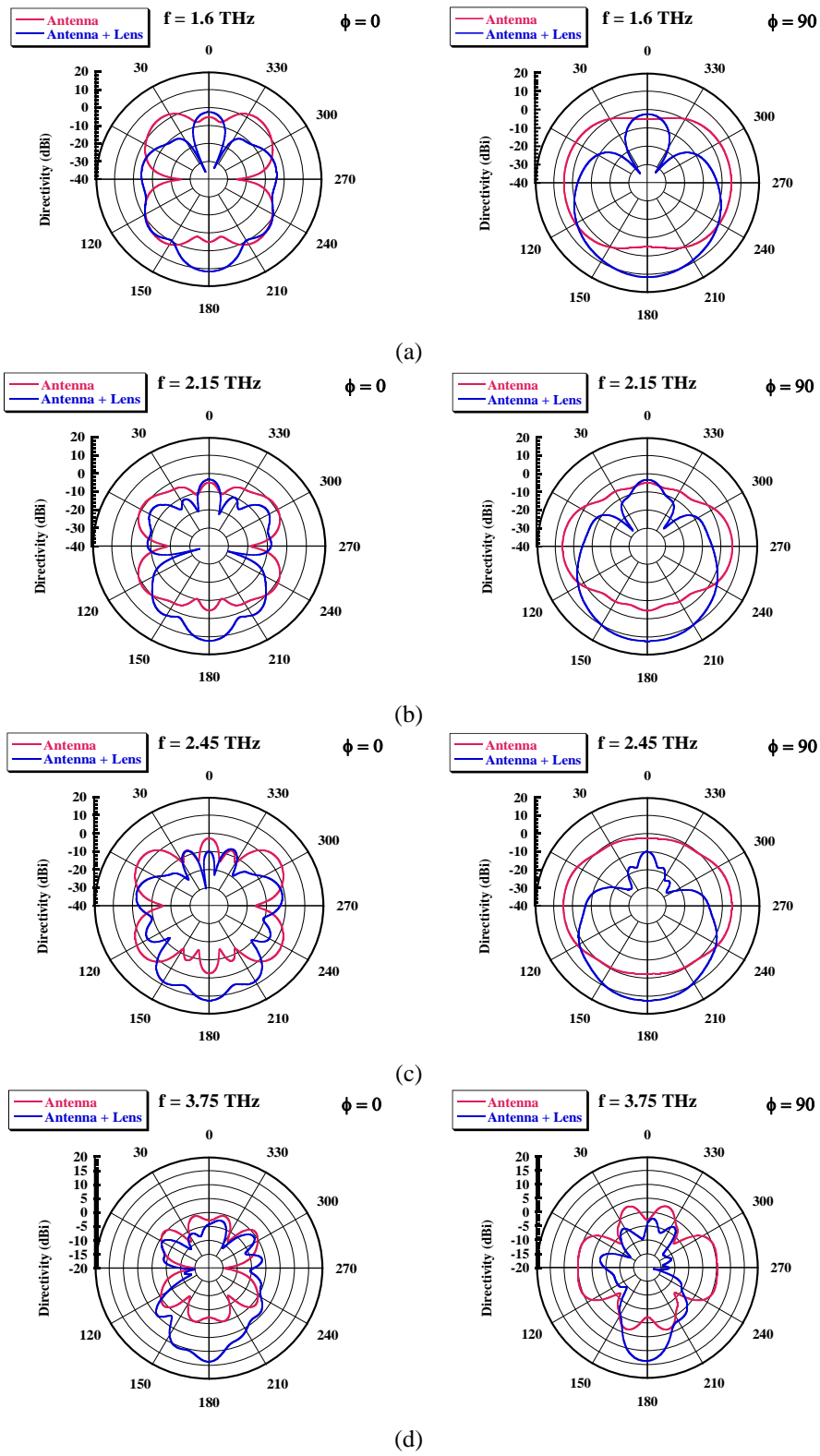
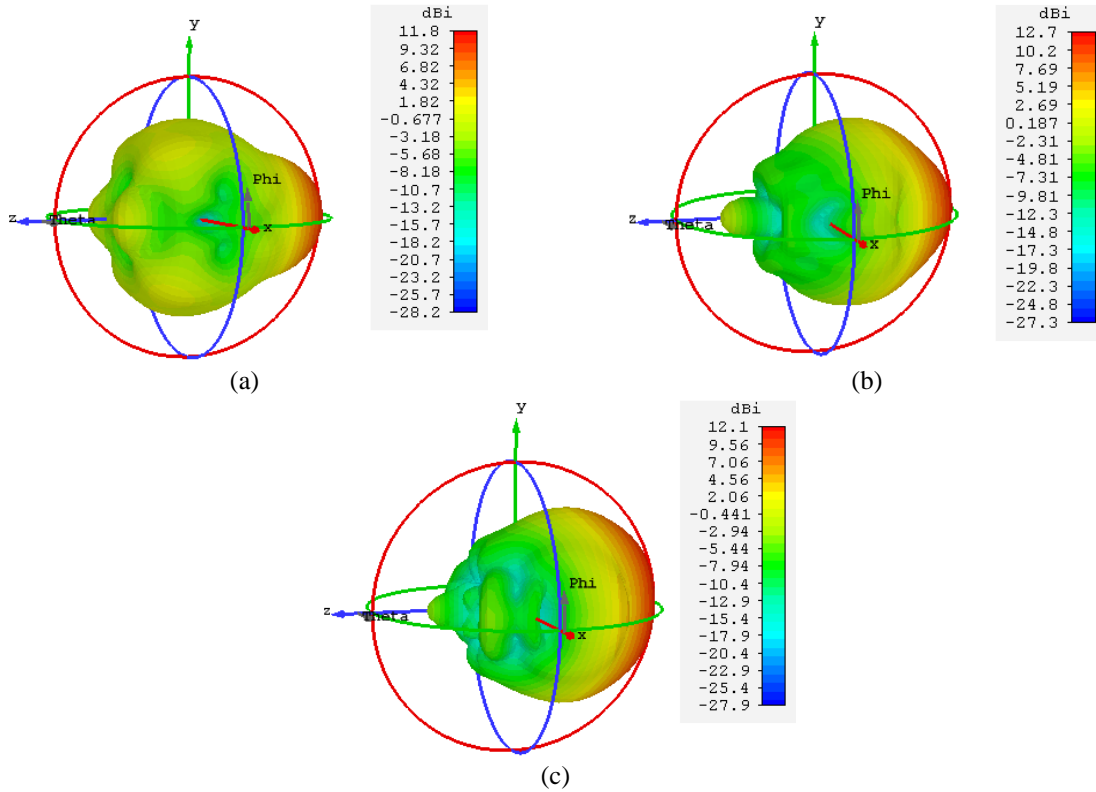Fig. 17. 2D Radiation patter for R_L =160 µm: (a) 1.75 THz, (b) 2.1 THz, (c) 3.8 THz, and (d) 4.5THz.

Fig. 18. 3D radiation patterns for different R_L values: (a) R_L = 80 µm at f = 2 THz, (b) R_L = 120 µm at f = 2.1 THz, and (c) R_L = 160 µm at f = 2.15 THz.

Table 6: Comparison of proposed UWB Bowtie PCA design with the legacy design

References	Antenna Type	Substrate	Antenna Electrode Material	Lens/FSS	-10 dB Impedance Bandwidth (THz)	Maximum Directivity (dBi)	3dB AR Bandwidth (THz)
Jyothi [12]	Bow-tie PCA	GaAs	TiAu /AuGe / AuCr	Si hemispherical lens	0.20	10.85	-
Malhotra [13]	Dipole planner array	LT-GaAs	Ti-Au	FSS	0.37	13.2	-
Gupta et al.[11]	Bow-tie PCA with dielectric coating	SI-GaAs	AuGe	HRFZ-Si lens	-	-	-
Zhu [15]	Bow-tie PCA	LT-GaAs	Ti-Au	No lens	0.18	8.0	-
	Bow-tie PCA			Si hemispherical lens		11.8	
	Bow-tie PCA with lens and combined with metasurface superstrate			FSS		11.9	
Han [14]	Yagi-uda	GaAs	Ti-Au	No lens	0.02	10.9	
Singh et al. [18]	Spiral-shaped	Si	Al	No lens	0.25	-	-
Formanek [10]	Dipole-type PCA	GaAs	Gold	Aspheric lens	0.80	-	-
Deva [17]	Conical horn	GaAs	-	Si-lens	-	18.5	-
Park [16]	Nanoplasmonic bow-tie PCA	GaAs	Cr/Au	No lens	1.00	-	-
Proposed Work	Bowtie	Quartz	Gold	Si hemispherical lens	3.00	18.2	6.00

IV. CONCLUSION

This research study has presented the full-wave numerical results of a wideband and high directivity bowtie PCA for THz frequency sensing and imaging applications. The detailed parametric analysis of the antenna design parameters was performed in CST MWS to obtain the optimal design parameters of the proposed antenna. The designed optimized bowtie PCA exhibits wideband impedance matching characteristics of 3 THz as well as 3 dB axial ratio bandwidth of 6 THz. The addition of the silicon lens with different diameters in the antenna structures increases its peak directivity to 18.2 dBi and overall efficiency of more than 55 % with peak value of 98% in the analyzed frequency band of 1 to 6 THz.

ACKNOWLEDGMENT

REFERENCES

[1] P. U. Jepsen, D. G. Cooke, and M. Koch, "Terahertz spectroscopy and imaging – Modern techniques and applications," *Laser & Photonics Reviews*, vol. 5, no. 1, pp. 124-166, 2011/01/03 2011.

[2] I. Kasalynas, R. Venckevicius, and G. Valusis, "Continuous wave spectroscopic terahertz imaging with InGaAs bow-tie diodes at room temperature," *IEEE Sensors Journal*, vol. 13, no. 1, pp. 50-54, 2013.

[3] Y. C. Shen, T. Lo, P. F. Taday, B. E. Cole, W. R. Tribe, and M. C. Kemp, "Detection and identification of explosives using terahertz pulsed spectroscopic imaging," *Applied Physics Letters*, vol. 86, no. 24, p. 241116, 2005/06/13 2005.

[4] G. Rana, *et al.*, "A polarization-resolved study of nanopatterned photoconductive antenna for enhanced terahertz emission," *IEEE Transactions on Terahertz Science and Technology*, vol. 9, no. 2, pp. 193-199, 2019.

[5] B. M. Fischer, M. Walther, and P. U. Jepsen, "Far-infrared vibrational modes of DNA components studied by terahertz time-domain spectroscopy," *Physics in Medicine and Biology*, vol. 47, no. 21, pp. 3807-3814, 2002/10/16 2002.

[6] K. Serita, *et al.*, "Scanning laser terahertz near-field imaging system," *Optics Express*, vol. 20, no. 12, pp. 12959-12965, 2012/06/04 2012.

[7] S. Yu, B. J. Drouin, and J. C. Pearson, "Terahertz spectroscopy of the bending vibrations of acetylene 12C2H2," *The Astrophysical Journal*, vol. 705, no. 1, pp. 786-790, 2009/10/15 2009.

[8] W. Zhang, A. K. Azad, and D. Grischkowsky, "Terahertz studies of carrier dynamics and dielectric response of n-type, freestanding epitaxial GaN," *Applied Physics Letters*, vol. 82, no. 17, pp. 2841-2843, 2003/04/28 2003.

[9] I. Malhotra, K. R. Jha, and G. Singh, "Terahertz antenna technology for imaging applications: A technical review," *International Journal of Microwave and Wireless Technologies*, vol. 10, no. 3, pp. 271-290, 2018.

[10] F. Formanek, M.-A. Brun, T. Umetsu, S. Omori, and A. Yasuda, "Aspheric silicon lenses for terahertz photoconductive antennas," *Applied Physics Letters*, vol. 94, no. 2, p. 021113, 2009/01/12 2009.

[11] A. Gupta, *et al.*, "Enhanced optical-to-THz conversion efficiency of photoconductive antenna using dielectric nano-layer encapsulation," *APL Photonics*, vol. 3, no. 5, p. 051706, 2018/05/01 2018.

[12] A. Jyothi, C. Saha, B. Ghosh, R. Kini, and C. Vaisakh, "Design of a gain enhanced THz bow-tie photoconductive antenna," in *2016 International Symposium on Antennas and Propagation (APSYM)*, pp. 1-3, 2016.

[13] I. Malhotra, K. R. Jha, and G. Singh, "Design of highly directive lens-less photoconductive dipole antenna array with frequency selective surface for terahertz imaging applications," *Optik*, vol. 173, pp. 206-219, 2018/11/01/ 2018.

[14] K. Han, Y. Park, S. Kim, H. Han, I. Park, and H. Lim, "A terahertz Yagi-Uda antenna for high input impedance," in *2008 33rd International Conference on Infrared, Millimeter and Terahertz Waves*, pp. 1-2, 2008.

[15] N. Zhu and R. W. Ziolkowski, "Photoconductive THz antenna designs with high radiation efficiency, high directivity, and high aperture efficiency," *IEEE Transactions on Terahertz Science and Technology*, vol. 3, no. 6, pp. 721-730, 2013.

[16] S.-G. Park, Y. Choi, Y.-J. Oh, and K.-H. Jeong, "Terahertz photoconductive antenna with metal nanoislands," *Optics Express*, vol. 20, no. 23, pp. 25530-25535, 2012/11/05 2012.

[17] U. Deva and C. Saha, "Gain enhancement of photoconductive THz antenna using conical GaAs horn and Si lens," in *2016 International Symposium on Antennas and Propagation (APSYM)*, pp. 1-3, 2016.

[18] R. Singh, *et al.*, "Spiral-type terahertz antennas and the manifestation of the Mushiake principle," *Optics Express*, vol. 17, no. 12, pp. 9971-9980, 2009/06/08 2009.

[19] C. Headley, *et al.*, "Improved performance of GaAs-based terahertz emitters via surface

passivation and silicon nitride encapsulation," *IEEE Journal of Selected Topics in Quantum Electronics*, vol. 17, no. 1, pp. 17-21, 2011.

[20] G. Matthäus, *et al.*, "Large-area microlens emitters for powerful THz emission," *Applied Physics B*, vol. 96, no. 2, pp. 233-235, 2009/08/01 2009.

[21] A. Singh and S. S. Prabhu, "Microlensless interdigitated photoconductive terahertz emitters," *Optics Express*, vol. 23, no. 2, pp. 1529-1535, 2015/01/26 2015.

[22] L. Hou and W. Shi, "An LT-GaAs terahertz photoconductive antenna with high emission power, low noise, and good stability," *IEEE Transactions on Electron Devices*, vol. 60, no. 5, pp. 1619-1624, 2013.

[23] A. Jooshesh, *et al.*, "Plasmon-enhanced LT-GaAs/AlAs heterostructure photoconductive antennas for sub-bandgap terahertz generation," *Optics Express*, vol. 25, no. 18, pp. 22140-22148, 2017/09/04 2017.

[24] N. M. Burford and M. O. El-Shenawee, *Review of Terahertz Photoconductive Antenna Technology* (no. 1, J. Optical Engineering), SPIE, pp. 1-20, 20, 2017.

[25] M. N. Hasan and M. Seo, "High-gain 2×2 UWB antenna array with integrated phase inverter," *Electronics Letters*, vol. 54, no. 10, pp. 612-614

[26] M. Amin, J. Yousaf, and S. Iqbal, "Single feed circularly polarised omnidirectional bifilar helix antennas with wide axial ratio beamwidth," *IET Microwaves, Antennas & Propagation*, vol. 7, no. 10, pp. 825-830, 2013.